Journal of Engineering Science and Technology
Vol. 7, No. 3 (2012) 360 - 378

ITERATIVE SOVA DECODING OVER SYMMETRIC ALPHA STABLE CHANNELS

CHUAN HSIAN, PU

American Degree Transfer Program, Taylor's University, Lakeside Campus,
No. 1 Jalan Taylor's, 47500, Subang Jaya, Selangor DE, Malaysia
*Corresponding Author: ChuanHsian.Pu@taylors.edu.my

Abstract

Soft-Output Viterbi Algorithm (SOVA) is one type of recovery memory-less Markov Chain and is used widely to decode convolutional codes. Fundamentally, conventional SOVA is designed on the basis of Maximum A-Posteriori probability (MAP) under Additive White Gaussian Noise (AWGN) interference. Therefore, the use of conventional Gaussian-based SOVA performs inefficiently and generates high BER (Bit Error Rate) in the presence of Symmetric Alpha Stable noise SαS. The poor performance of the Gaussian-based SOVA can be attributed to the mathematical quadratic cost function of the receiving mechanism. The quadratic cost function at the receiving end is statistically vulnerable and inefficient to guard SOVA component decoder against the entries of the outliers which are superimposed on the transmitted signal from hostile SαS channel. The author studies and improves the performance of conventional SOVA with the introduction of Bayesian Cauchy metric calculation. Substantial performance improvement was observed from Mento Carlo Simulation for SOVA running on the platform of parallel turbo codes.

Keywords: Soft output Viterbi algorithm (SOVA), Symmetric alpha stable noise, Bayesian Cauchy metric and Non-Gaussian channel.

1. Introduction

Iterative decoding of turbo codes has received a lot attentions from researchers since its invention and has proven to approach Shannon capacity asymptote with required E_b/N_o of 0.7 dB for BER of 10^{-5} [1-3]. After more than a decade of its first publication, the practical use of turbo codes have commenced [4] and various modern communication devices begin to enjoy the unbelievable decoding

Nomenclatures

$A_k(s_k)$	LOG-MAP LLR forward probabilistic recursion
$B_{k+1}(s_{k+1})$	LOG-MAP LLR backward probabilistic recursion
E_b/N_o	Bit energy to noise spectral density ratio
$L_e(u_k)$	Extrinsic LLR
$L_e(u_i\|y)$	APP log-likelihood ratio (LLR)
$L_1(u_k)$	Priori LLR
$M(s_k)$	Path-metric at time instant k
$P(s_k)$	Probability at time instant k
s_k	State of trellis at time instant k

Greek Symbols

α	Characteristic exponent
Δ_k^s	Path metric difference at state s and at time instant k
$\phi(\omega)$	Characteristic function
γ	Dispersion

Abbreviations

APP	A posteriori probability
AWGN	Additive white Gaussian noise
BER	Bit error rate
LLR	Log-likelihood ratio
MAP	Maximum a posteriori probability
PCCC	Parallel concatenated convolutional codes/turbo codes
SCCC	Serial concatenated convolutional codes/turbo codes
SOVA	Soft output Viterbi algorithm
SαS	Symmetric alpha stable distribution
VA	Viterbi algorithm
RSC	Recursive systematic convolutional codes

performance brought by turbo codes. The excited development of turbo codes are fuelled by the belief that all type of channels induce impairment could be resolved with turbo like codes as long as code rate does not exceed Shannon predicted limit, hence, such trend and belief further triggered the exploration of 'turbo-like codes' in various stages of digital communication such as source coding, channel coding, equalization, coded modulation, multiple access systems, etc. [5]. Typically, turbo codes can be viewed as the parallel or serial concatenation of two or more convolutional codes. It works on the principle of memoryless Markov-Chain where performance is improved in subsequent iteration by passing probabilistic message gleaning from previous iterations to achieve Shannon's capacity asymptote. The design of the turbo codes and its performance are basically lying on the foundation of normal distribution. Gaussian noise is deemed the default interference to the transmitted signal over dispersive transmission medium. Therefore, conventional turbo codes are

optimized for AWGN channels. Generally, AWGN channels exhibit normal distribution and has uniform power spectral density N_o which equally interfere the entire bandwidth of consideration.

With the rapid development of modern digital communication technologies, such assumption is no longer sufficient for the applications of turbo codes in hostile environment which transmitted signal is experiencing non-Gaussian impulsive noise on top of AWGN in impulsive communication links. Power line communication channel, digital subscriber line, indoor radio channels, underwater acoustic channel and etc. are the examples of impulsive communication links [6-8]. In the presence of non-Gaussian noise, the performance of conventional turbo codes is found substantially degraded [9] due to the heavy tailed distribution of the impulsive noise. Various researches have been devoted so far to overcome the detrimental effects of impulsive noise such as introducing non-linear pre-processor to filter or suppress the received signal without changing the internal matched filtering mechanism of turbo codes [5, 10-13], apply Huber metric or introducing robust Middleton's Class A measurement in branch metric computation to suppress the entries of impulsive outliers from channel respectively [14].

The malfunction of Gaussian-based detector in impulsive noise was investigated and several solutions were proposed in previous works to remedy the impairments caused to the Gaussian-optimized turbo codes. Hard-decision p-norm was used to improve the branch metric computation [15]. Subsequently, absolute branch metric was proposed in for Viterbi decoding and its theoretical BER bound was derived [16]. Practical BER performance for absolute branch metric and suboptimal system were proposed and analysed for Viterbi decoder in [17]. A Cauchy-based detection was proposed for MAP turbo codes in turbo-coded FH M-FSK ad hoc packet radio networks [18]. Another further development was proposed for non-coherent receiver and substantial performance improvement was reported [19]. The successful implementation of Cauchy model in probabilistic branch metric computation has enable MAP turbo codes to operate effectively under Symmetric Alpha Stable ($S\alpha S$) impulsive noise interference. Recently, a numerical probability branch metric has been proposed to cover all cases of alpha α values (except $\alpha=1$ Cauchy and $\alpha=2$ Gaussian distributions) where no closed form solutions are available for computation and approximation of Riemann sum was used to determine branch metric numerically in [20]. In view of the high complexity of MAP turbo codes which is practically infeasible for hardware implementation, the author further extended the works done on MAP turbo codes and incorporates the robust Cauchy-based model into SOVA component decoder to find a practically less-complicated solution for robust detection over $S\alpha S$ channel.

The paper is organized as follows: In section 2.1, a brief overview of turbo codes and channel model are given, section 2.2 shows the statistical noise model used to describe the impulsive noise and section 2.3 describes a mathematical model of SOVA decoding and proposes the workable solution to incorporate robust Cauchy metric into existing SOVA component decoders. Finally, section 3 presented various simulation results collected through Monte Carlo simulation for proposed robust SOVA decoders and conclusions are drawn in section 5.

2. System Description and Channel Model

2.1. Parallel turbo codes structure

Typically, turbo codes can be categorized according to its concatenated connections, which are parallel concatenated convolutional codes (PCCC) and serial concatenated convolutional codes (SCCC). PCCC is achieved by wiring the component encoders in parallel likewise to SCCC where component encoders are wired in serial fashion [3, 21, 22]. PCCC is used as the platform in our analysis to obtain the performance of conventional SOVA [23] and robust SOVA for both AWGN and SαS investigation. The structure of PCCC encoder is illustrated as Fig. 1:

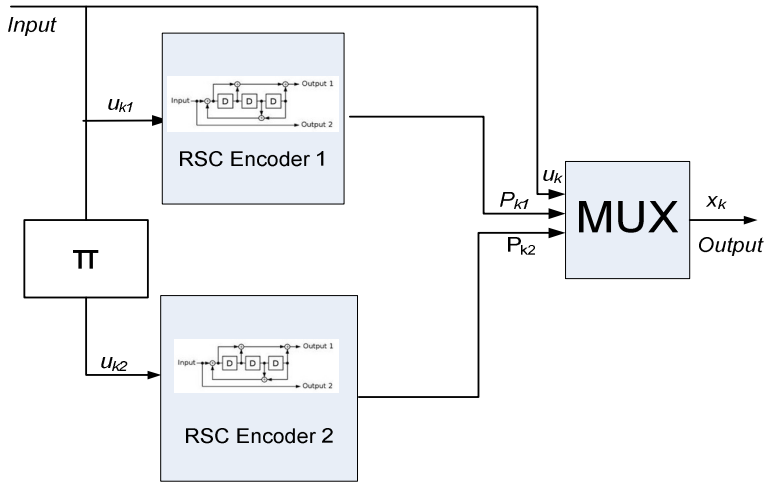

Fig. 1. PCCC Encoder with Code Rate *r* = 1/3.

The encoder of parallel turbo codes consists of two parallel recursive systematic convolutional (RSC) encoders with the random interleaver π. The binary information $\{u_k = \pm 1\}_1^n$ is fed into the parallel RSC encoders. The scrambled bits u_{k2} are sent to second RSC encoder. Random interleaver π is used in turbo codes to minimize the symbol correlation between two inputs u_{k1} and u_{k2}. Coded output bit stream $\{x_1 = \pm 1\}_1^L$ is produced by multiplexing the parity bits p_{k1} and p_{k2} from the parallel RSC encoders together with the systematic bits u_k from the input.

Typically, the code rate of the parallel RSC encoders can be defined in Eq. (1)

$$R = \frac{k}{n} \tag{1}$$

where k is the information bits and n is the output bits. To increase the data rate, puncturing can be performed on first and second parity bits at two RSC encoders alternatively prior to multiplexing.

The coded bit stream can be decoded iteratively with SOVA decoder in PCCC. The SOVA decoder of PCCC is illustrated as Fig. 2:

The transmitted bit stream $\mathbf{x}$ of the PCCC are sent over transmission medium within baseband spectrum in our simulation with the assumption that the transmission medium is experiencing interference from Additive White Gaussian Noise (AWGN) or SαS noise interferences. The received information $\{y_k = \pm 1\}_1^L$ which has been corrupted by AWGN and SαS noises would be decoded iteratively with SOVA decoder after matched filter. SOVA decoder exploits the parity information embedded into the information bits for errors detection and correction. Soft information is used instead of hard-decision information to serve as priori information $L_1(u_k)$ and $L_2(u_k)$ to improve the current bit estimates. From Fig. 2, it is shown that extrinsic information $L_{e1}(u_k)$ and $L_{e2}(u_k)$ could be obtained by subtracting the soft a-posteriori-probability (APP) outputs $L_1(u_k|\mathbf{y})$ and $L_2(u_k|\mathbf{y})$ from systematic LLRs $L_c(y_{ks})$ and priori information $L_1(u_k)$ and $L_2(u_k)$ respectively. The extrinsic information $L_e(u_k)$ from decoder 1 is sent to their counterpart as priori information $L(u_k)$ to aid and improve the estimation of the APP output $L(u_k|\mathbf{y})$ for decoder 2 and vice-versa in iterative manner. Finally, hard-decision decoded bits d_k are generated from the second SOVA component decoder with signum function in each completion of iteration process.

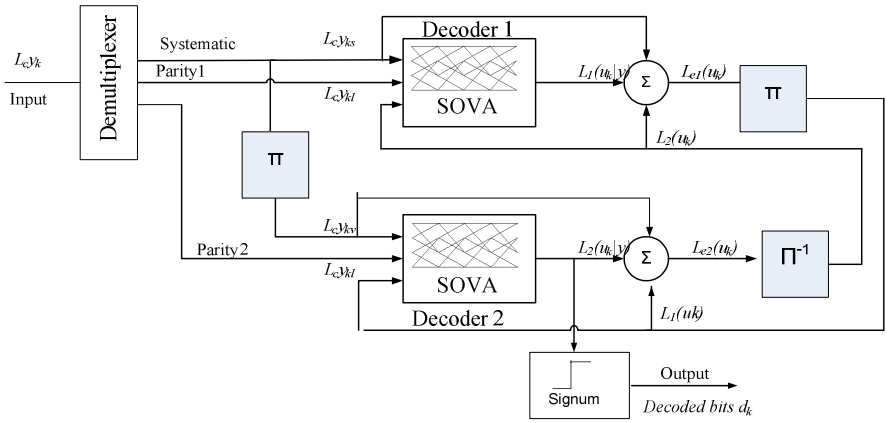

Fig. 2. SOVA Decoder for PCCC.

Burst errors from the dispersive channel could be randomised with interleaver at the decoder. Hence, due to the interleaving and de-interleaving processes, burst errors from the received sequence are spread to achieve statistical independent on the received bit stream.

Since soft-output extrinsic information $L_e(u)$ is exchanged between the component RSC decoders and better estimation is obtained for additional iteration of turbo codes. Typically, the BER of the decoded bits will fall exponentially in each incremental 'turbo' processing and has the BER curve resembles 'waterfall'. Generally, each iteration that is performed; the performance improvement is also decrease exponentially. For reasonable complexity and acceptable decoding latency, eight iterations are suggested because after eight iterations, additional iteration shows insignificant improvement over LLR decoded bits [24].

2.2. Symmetric alpha-stable (SαS) noise model

Power line communication (PLC), digital subscriber loop, indoor radio channel or underwater acoustic links have been the fascinating topics and active fields of researches. However, the design of such transmission links required the consideration of the impairments from impulsive noise and AWGN noise. Conventional channel codes are typically optimized for AWGN channel. In order to investigate non-Gaussian channel, statistical channel models are often serving as the indispensable platform to emulate the statistical noisy behaviour of environment for particular communication link.

To ease simulation and theoretical calculations, several statistical noise models have been developed for the purposes. They are contaminated Gaussian model, Generalized Gaussian Distribution (GCD), Stable Distributions and Middleton's Class. Symmetric Alpha-Stable model (SαS) [15, 25] is chosen to emulate the statistical impulsive nature of the impulsive noise. The reason for choosing symmetric Alpha Stable (SαS) model in our investigation is due to its excellent empirical fits on data and many signal processing applications are symmetrical in its statistical distribution. Typically, SαS distribution is characterized by setting its skewness parameter δ to zero. Its characteristic function is given in Eq. (2)

$$\phi(\omega) = e^{-\gamma^{\alpha}|\omega|^{\alpha}}, \qquad -\infty < \omega < \infty \tag{2}$$

where γ is dispersion and $\alpha \in (0, 2]$ is the characteristic exponent which described the impulsiveness of SαS process. When $\alpha = 2$, it gives Gaussian distribution and if $\alpha = 1$, Cauchy distribution could be obtained from the random process. Due to the non-close form for other values of α, our investigation is limited from $\alpha = 1$ to $\alpha = 2$. The SαS random process is simulated with different α values as given in Fig. 3 for $\alpha = 1$, 1.5, 1.7 and 2.

From Fig. 3, it can be observed that the parameter α determines the impulsiveness of the Symmetric Alpha-stable random variables. Typically, the smaller the value of α would result in the increasing impulsiveness for SαS process. Hence, the spikes on the Fig. 3 would appear to be sharper and more prevalent.

AWGN noise and SαS are added and superimposed on the received vector $\{y_k = \pm 1\}_1^L$ linearly and directly attenuate and distort the amplitude of the transmitted symbols in baseband model. Mathematically, it can be described with Eq. (3)

$$\mathbf{y} = A\sqrt{E_b}(2\mathbf{x} - 1) + \mathbf{n}_s + \mathbf{n}_w \tag{3}$$

where A is the channel gain or attenuation, E_b is bit energy and $\mathbf{n}_s$ and $\mathbf{n}_w$ are the SαS and AWGN random processes respectively.

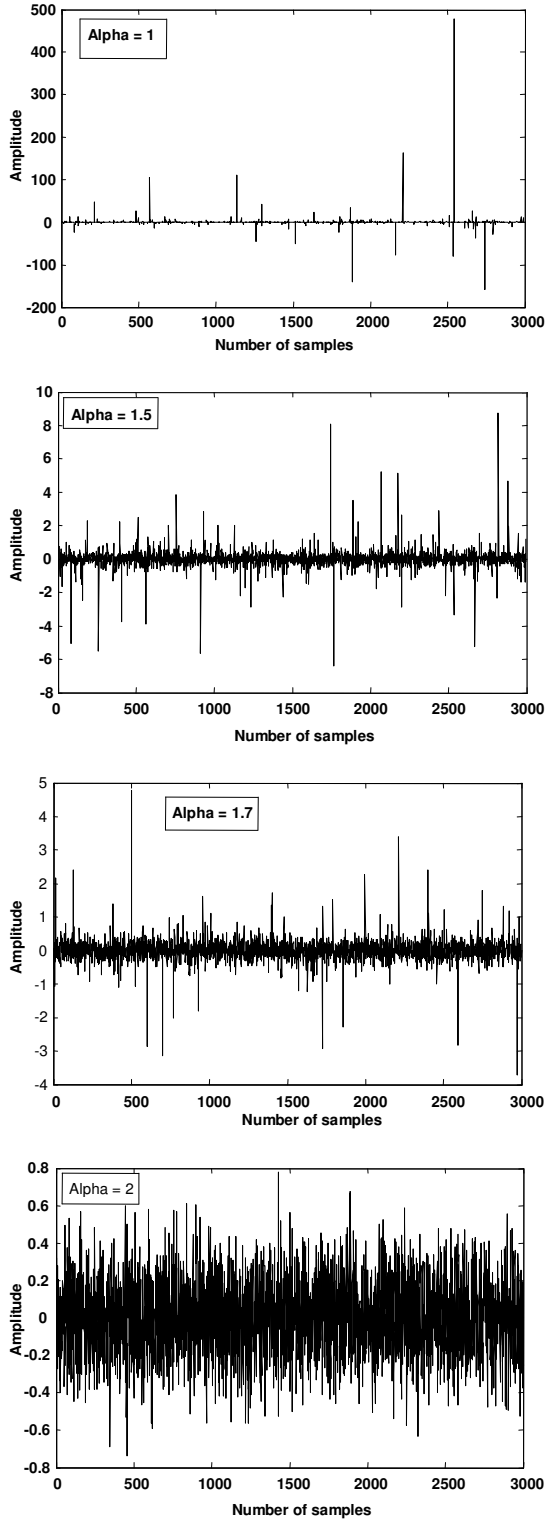

Fig. 3. Symmetric Alpha-Stable Noise with α = 1, 1.5, 1.7 and 2.

2.3. SOVA decoder and proposed improvements

2.3.1. Conventional Gaussian-based SOVA algorithm

Theoretically, SOVA is derived based on Maximum A posteriori (MAP) Estimation by incorporating soft decision information to the Viterbi algorithm (VA) to provide soft –decision output. MLE can be expressed mathematically as Eq. (4) which maximizes the a-posteriori probability (APP) of the decoded bits:

$$\begin{aligned}\hat{u} &= \arg\max\{p(\mathbf{u}\,|\,\mathbf{y})\} \\ &= \arg\max\{p(\mathbf{y}\,|\,\mathbf{u})p(\mathbf{u})\}\end{aligned} \tag{4}$$

The following equations for conventional and modified robust SOVA are based on the Equations and notations from [24]. The soft-decision output of SOVA is given as a-posteriori (APP) Log-Likelihood Ratio (LLR) as Eq. (5):

$$L(u_k\,|\,\mathbf{y}) = \ln\left(\frac{P(u_k)=+1\,|\,\mathbf{y}}{P(u_k)=-1\,|\,\mathbf{y}}\right) \tag{5}$$

Equation 5 above can be computed recursively by incorporating trellis as follows:

$$L(u_i\,|\,\mathbf{y}) = \ln\left(\frac{\sum_{u_i=+1} P(s_{k-1}, s_k, \mathbf{y})}{\sum_{u_i=-1} P(s_{k-1}, s_k, \mathbf{y})}\right) \tag{6}$$

$$L(u_k\,|\,\mathbf{y}) = \ln\left(\frac{\sum_{u_i=+1} \alpha_{k-1}(s_{k-1})\cdot\gamma_k(s_{k-1}, s_k)\cdot\beta_k(s_k)}{\sum_{u_i=-1} \alpha_{k-1}(s_{k-1})\cdot\gamma_k(s_{k-1}, s_k)\cdot\beta_k(s_k)}\right) \tag{7}$$

where u_k =+1 is fed to the SOVA component decoders that caused transition from previous state s_{k-1} to the present state s_k. For given u_k = -1, the component decoders are moving from s_{k-1} to the present state s_k. $\alpha_{k-1}(s_{k-1})$ is denoted as forward recursion. $\gamma_{k-1}(s_{k-1}, s_k)$ is denoted as the branch metric of trellis from state transition s_{k-1} to s_k and $B_k(s_k)$ is backward recursion.

To reduce the complexity of calculation, the APP-LLR from Eq. (7) can be computed recursively in natural logarithmic domain as Eq. (8):

$$L(u_k\,|\,\mathbf{y}) = \ln\left(\frac{\sum_{\substack{(s',s)\Rightarrow \\ u_k=+1}} \exp\left(\Gamma_k(s',s) + A_{k-1}(s') + B_k(s)\right)}{\sum_{\substack{(s',s)\Rightarrow \\ u_k=-1}} \exp\left(\Gamma_k(s',s) + A_{k-1}(s') + B_k(s)\right)}\right) \tag{8}$$

where

$A_k(s_k) = \ln\left(\alpha_{k-1}(s_{k-1})\cdot\gamma_k(s_{k-1}, s_k)\right)$ is forward probabilistic LLR recursion.

$B_{k+1}(s_{k+1}) = \ln\left(\beta_k(s_k)\cdot\gamma_k(s_{k-1}, s_k)\right)$ is backward probabilistic LLR recursion.

$\Gamma_k(s_{k-1}, s_k) = \ln\left(\gamma_k(s_{k-1}, s_k)\right)$ is the probabilistic LLR branch transition metric.

From Eq. (8), the branch transition metric can be obtained from Log-MAP APP as Eq. (9):

$$\Gamma_k(s_{k-1}, s_k) = \ln\{\gamma_k(s_{k-1}, s_k)\} = \hat{C} + \frac{1}{2}u_k L(u_k) + \frac{L_c}{2}\sum_{l=1}^{n}(y_{kl} \cdot x_{kl}) \tag{9}$$

where $L_c = 4\alpha\frac{E_b}{\sigma^2}$ is the channel reliability value which depends only on the E_b/N_o. Therefore, the branch transition metric can be obtained from the a-priori probability term of the input symbols $u_k L(u_k)$ and the channel measurement $y_{kl} \cdot x_{kl}$. The recursive form of path-metric can be derived as Eq. (10)

$$\begin{aligned} M(s_k) &= \ln\{p(s_k, y_{j\le k})\} = \ln\{p(s_{k-1}, y_{j\le k-1}, s_k, y_k)\} \\ &= M(s_{k-1}) + \ln\{p(y_k \mid s_k, s_{k-1})\} + \ln\{p(s_k \mid s_{k-1})\} \\ &= M(s_{k-1}) + \frac{1}{2}u_k L(u_k) + \frac{L_c}{2}\sum_{l=1}^{n}(y_{kl} \cdot x_{kl}) \end{aligned} \tag{10}$$

From Eq. (10), it shows that the path-metric can be updated recursively by adding a-priori term and channel measurement. The probability of making the correct decision to select path s_k instead of the merging path $\hat{s}_k$ can be given in Eq. (11).

$$P(\text{correct decision at } S_k = s) = \frac{P(s_k)}{P(s_k) + P(\hat{s}_k)} = \frac{e^{M(s_k)}}{e^{M(s_k)} + e^{M(\hat{s}_k)}} = \frac{e^{\Delta_k^{s_i}}}{1 + e^{\Delta_k^{s_i}}} \tag{11}$$

The soft output can be produced by considering the values of metric difference $\Delta_k^{s_i}$ for all state s_i along the maximum likelihood path from trellis stage $i=k$ to $i=k+\delta$ and is shown in [24] that this LLR could be approximated by Eq. (12).

$$LLR = L(u_k \mid y) \approx u_k \cdot \min_{\substack{i=k.....k+\delta \\ u_k \neq uk}} \Delta_k^{s_i} \tag{12}$$

where δ is traceback length and is typically set to five times the constraint length of decoding window for acceptable decoding latency as stated in [24].

2.3.2. Robust SOVA decoder with Cauchy-based metric

The performance improvement was achieved by modifying its branch metric with Bayesian Cauchy metric. The Cauchy metric was incorporated into its branch metric calculation for MAP (Maximum a-posteriori) PCCC decoder as reported in [18]. The use of Cauchy metric that was reported can increase the robustness of MAP decoder so that it can operate under impulsive noise environment without succumbing to the detrimental residuals from impulsive noise. However, MAP decoder is highly complicated for physical hardware realization and incurring decoding delay which is prohibited for time critical transmission. Hence, SOVA was introduced to give better performance and speed of decoding with lower hardware complexity [23].

Cauchy metric is obtained from Cauchy distribution as Eq. (13)

$$f(y) = \frac{1}{\pi}\frac{\gamma}{\gamma^2 + (y-x)^2} \tag{13}$$

with Cauchy Density Function (γ, β), where γ is the dispersion parameter and it relates to variance as $\sigma^2=2\gamma$. Hence the conditional probability of the received symbol can be expressed as

$$p(\mathbf{y_k} \mid \mathbf{x_k}) = \prod_{l=1}^{N} \frac{1}{2\pi} \frac{\gamma}{\left[\gamma^2 + (y_{kl} - a \cdot x_{kl})^2\right]^{\frac{3}{2}}} \tag{14}$$

where a is the fading amplitude of the channel where $a = 1$ for non-fading AWGN channel. To enable the effective decoding of SOVA in impulsive noise, modification on the branch metric of conventional Gaussian based-SOVA is needed for robust detection. To equip the conventional SOVA decoder for robustness, the pathmetric could be modified as Eq. (15)

$$M(s_k) = \ln\{p(s_k, y_{j\le k})\} = M(s_{k-1}) + \ln\{p(y_k \mid s_k, s_{k-1})\} + \ln\{p(s_k \mid s_{k-1})\} \tag{15}$$

where $p(s_k \mid s_{k-1}) = p(u_k)$ is the priori probability of the input bit $u_k = \pm 1$ and $p(y_k \mid s_{k-1}, s_k) = p(y_k, x_k)$. Hence, the accumulated path-metric $M(s_k^s)$ that can be computed recursively with the incorporation of the Cauchy distribution from Eq. (14) into Eq. (15) and produces the Eq. (16) for robust detection:

$$M(s) = C_1 + M(s_{k-1}) + \frac{u_k L(u_k)}{2} - \frac{3}{2}\sum_{l=1}^{n} \ln\left(\gamma^2 + (y_{kl} - a x_{kl})^2\right) \tag{16}$$

where constant $C_1 = N \ln\left(\frac{\gamma}{2\pi}\right)$ can be omitted. If two paths merge at state s_k, then path s_k is selected on the basis that $M(s_k) > M(\hat{s}_k)$. Equation (16) can be simplified as follows:

$$\begin{aligned} M(s_k) &= C_1 + M(s_{k-1}) + \frac{u_k L(u_k)}{2} + \frac{3}{2}\sum_{l=1}^{n} \ln\left(\gamma^2 + y_{kl}^2 + (a x_{kl})^2 - 2 a x_{kl} y_{kl}\right) \\ &= C_1 + M(s_{k-1}) + \frac{u_k L(u_k)}{2} + \frac{3}{2}\sum_{l=1}^{n} \ln(C_2 - 2 a x_{kl} y_{kl}) \end{aligned} \tag{17}$$

where $C_2 = \gamma^2 + y_{kl}^2 + (a x_{kl})^2$. From Eq. (17), it is easily observed that Cauchy density function from Eq. (14) is incorporated into branch transition metric from Eq. (15). Hence, such modification to branch metric $\gamma(s_{k-1}, s_k)$ could improve the robustness of SOVA. The performance improvement could be attributed to the monotonic increment characteristics of logarithmic function which suppresses the large input as the input gradually increases.

Then the path metric difference Δ_k^s of the merging path at stage k can be determined which is served as the magnitude of the soft-decision output of robust SOVA as the Eq. (18)

$$\Delta_k^s = M(s_k) - M(\hat{s}_k) \ge 0 \tag{18}$$

Hence, the soft-decision output of robust SOVA can be expressed as Eq. (19) for optimal performance.

$$L(u_k \mid y_k) = u_k \cdot \min_{\substack{j=k,\ldots,n \\ u_k \ne u_k^{jk}}} \Delta_k^s \tag{19}$$

The extrinsic information $L_e(\mathbf{u})$ could be obtained mathematically as Eq. (20).

$$L_e(u_k) = L(u_k \mid y) - L(u_k) - L_{sys}(u_k) \tag{20}$$

where $L_{sys} = \frac{3}{2}\{\ln(C_2 + 2y_{ks}) - \ln(C_2 - 2y_{ks})\} \cdot L(u_k)$ is the priori LLR from information bits and $L_{sys}(u_k)$ is the LLR from systematic bits of the received signal. Finally, the hard decoded bits can be obtained mathematically from second SOVA component decoder LLRs output as Eq. (19)

$$\hat{u}_k = \frac{\text{sgn}(L(u_k \mid y)) + 1}{2} \tag{21}$$

where sgn(x) is a signum function.

3. Results and Discussion

Mento Carlo simulation was performed on the modified robust SOVA PCCC over impulsive SαS channel. Numerical results were collected and analysed. In our simulation, binary information bits with 1000 bits and 100 frames were encoded with parallel convolutional encoder with un-punctured rate $r = 1/3$. Subsequently, it is transmitted directly as baseband signal over noisy transmission medium. We investigate both AWGN and SαS channels. The performance of conventional Gaussian-based SOVA and the proposed Cauchy-Based SOVA were tested on the configuration of PCCC. Table 1 below gives the simulation parameters used in the Mento Carlo method to investigate our robust Cauchy-Based turbo codes.

Table1. Turbo Encoder and Decoder Parameters used in Mento Carlo Simulation.

Channel Noise	**Symmetric alpha-stable SαS noise where α = 1 (Cauchy), 1.5, 1.7 and 2 (Gaussian).**
Component decoders	Two identical Recursive Systematic Convolutional (RSC) Encoders. Code rate R = 1/3, G_o=7_8, G_1=5_8
Interleaver	1000 bit random interleaver.
Number of iterations	8 Iterations.
APP Decoding algorithms	Bayesian Gaussian-based conventional SOVA, Bayesian Cauchy-based robust SOVA and Bayesian Cauchy-based Log MAP algorithms.
Traceback length	30

In the simulation results given below, heuristic approach is used to show the robustness of the proposed Cauchy-based robust SOVA decoder and comparisons are made against the Gaussian-based conventional SOVA decoder. Eight iterations were performed in the following investigation for the optimum performance of the turbo codes without introducing significant decoding delay for efficiency.

First of all, we examine the soft-decision APP LLR Output of the Gaussian-based SOVA decoder that performs over AWGN channels as shown in Fig. 4. The LLR outputs from the second Gaussian-based SOVA component decoders are used in the following figures. The vertical axis of each subplot represents the decoded LLR bits and horizontal axis represents number bits used. Assuming that all zero

sequence was convolutionally encoded with PCCC and be sent over AWGN channel with E_b/N_o = 1 dB. As the number of iterations increased as in Fig 4, the LLR outputs gradually converge after 8 iterations and less ambiguous outputs produced comparable to first and second iterations. Hence Gaussian-based SOVA decoders can perform effectively to correct bit symbol errors in AWGN noise.

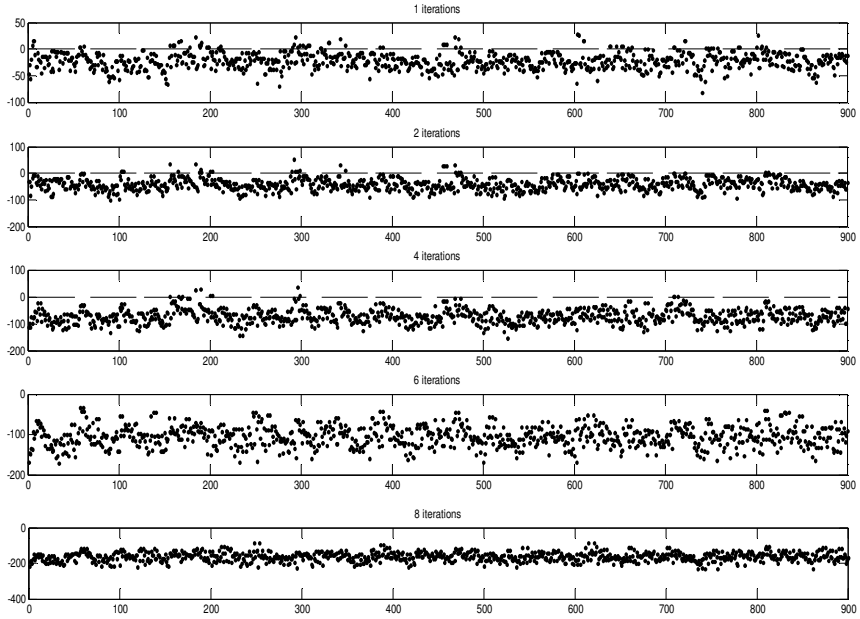

Fig. 4. Decoded soft LLR Output of Gaussian-Based SOVA over AWGN Channel at E_b/N_o = 1 dB.

Subsequently, the same Gaussian-based SOVA component decoders were tested in $S\alpha S$ noise with α = 1 (Cauchy distribution), which the noise sequence follows Cauchy distribution with the presence of impulsive outliers. The heuristic result is shown in Fig. 5, there is no performance improvement is gleaned throughout 8 iterations performed. The malfunction of Gaussian-based SOVA component decoders could be attributed to the presence of detrimental residuals that disrupted the proper decoding operation of Gaussian-based component decoders running on Euclidean metric. Such outliers typically possess spiky amplitude with the rate of arrival following Poisson distribution. Hence, iterative process of Gaussian-based SOVA could not benefit from such hostile noise transmission as the spiky outliers could cause more erroneous decisions on the pair of SOVA component decoders. This is because Euclidean metric with quadratic computation has the tendency to succumb to large amplitude outliers statistically as it was mathematically described in Section 2.3.1. In addition, due to the 'turbo' decoding procedure, extrinsic information is exchanged during iterative decoding process further worsening the outcome.

Figure 6 shows the performance of proposed Cauchy-based SOVA parallel decoder in the presence of identical SαS noise interference with α=1and operated at E_b/N_o = 8 dB. Robust detection and correction were achieved with the use of Cauchy-based metric as proposed in section instead of matched filtering detection

in conventional turbo codes in AWGN noise. However, due to the impulsiveness and spiky received sequence, performance improvement could only be observed at higher E_b/N_o threshold. As robust SOVA component decoders need to operate at higher E_b/N_o threshold to achieve good performance and such phenomena could be observed from the BER analysis in the following figures.

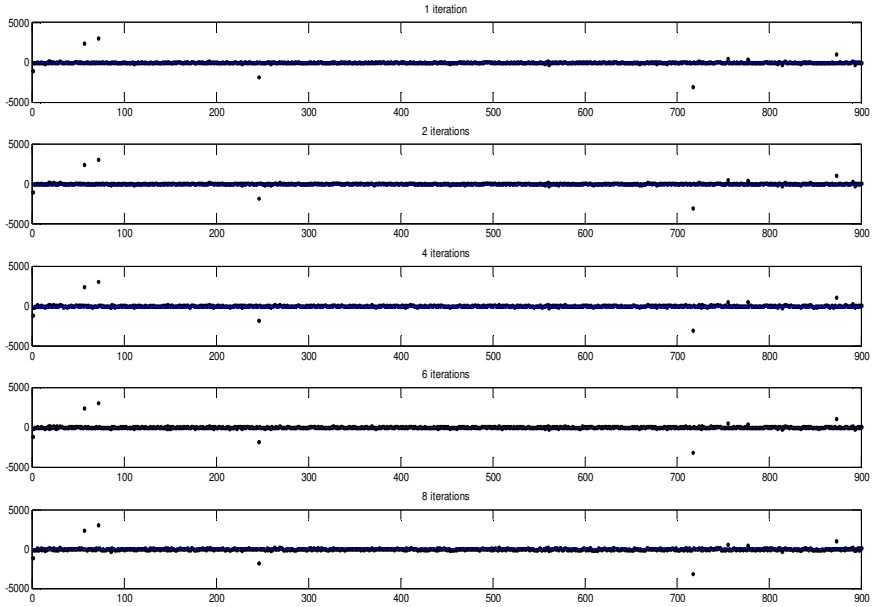

Fig. 5 Decoded soft LLR Output of Gaussian-based SOVA over SαS Channel with $\alpha = 1$ at E_b/N_o = 8 dB.

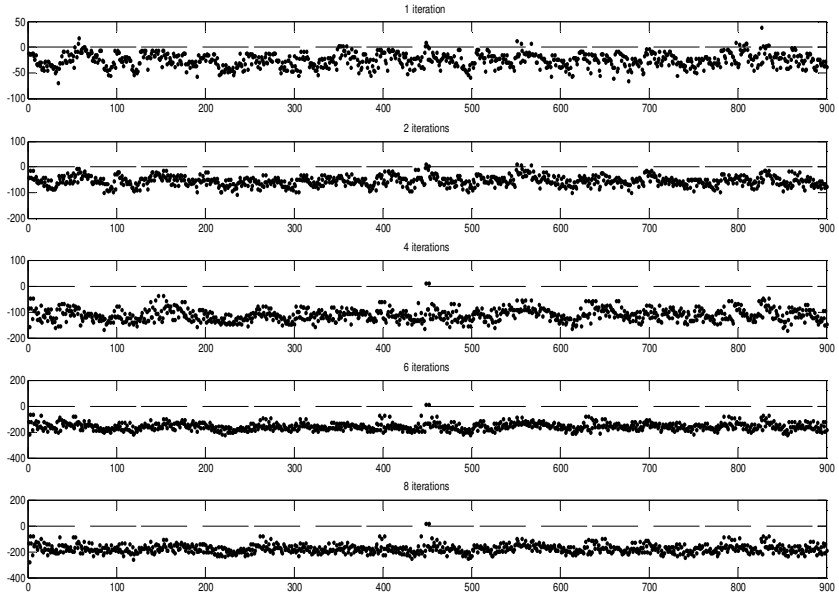

Fig. 6. Decoded Soft LLR Output of Cauchy-Based SOVA over SαS Channel with $\alpha = 1$ at E_b/N_o = 8 dB.

3.1. Performance in AWGN noise with Bayesian Gaussian metric

Ultimately, the performance of the proposed SOVA was analysed in term of BER and E_b/N_o for clearer picture of its effectiveness against disruptive outliers from the impulsive noise. Again, the performance of Gaussian-based SOVA in its parallel configuration was plotted in Fig. 7 for eight iterations for ease of comparison.

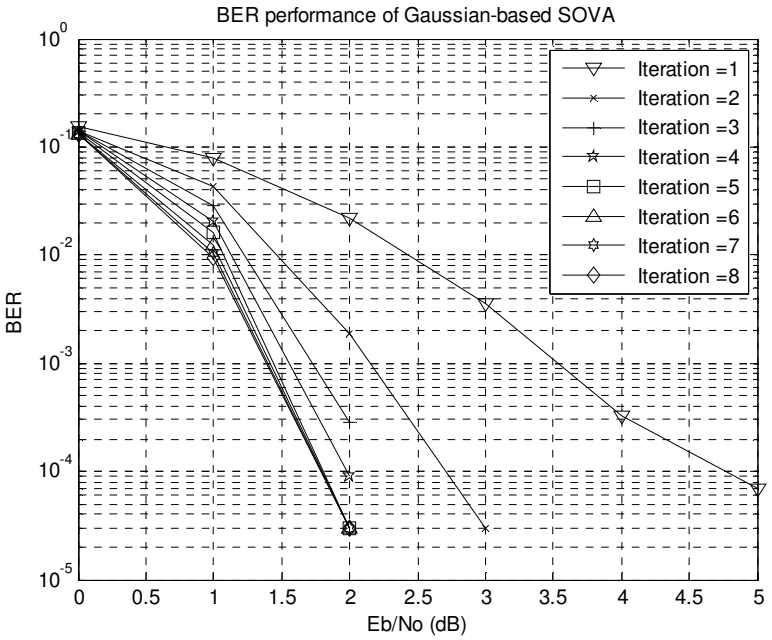

Fig. 7. BER Performance for Conventional SOVA with Bayesian Gaussian metric over AWGN Channel.

From the Fig. 7, it is shown that Gaussian-based SOVA could reduce the probability of errors as the numbers of iteration increase. Shannon Capacity Limit is gradually approached if more than 8 iterations are performed on the received data bits in AWGN noise.

3.2. Performance in $S\alpha S$ noise with Bayesian Gaussian metric

However, significant performance degradation can be observed from Fig. 8 while Gaussian-based SOVA attempted to correct errors due to SαS noise with α=1. The increment of the iterations is helplessly to improve the BER performance of conventional turbo codes in the presence of outliers. This is because the outliers could drastically bias the estimates of quadratic type Gaussian-based matched filter at the receiving end. Furthermore, the exchanging of extrinsic information L_e between the two components SOVA component decoders further degrade the BER performance as harmful and detrimental information were gleaned as L_e that cause more erroneous decoding.

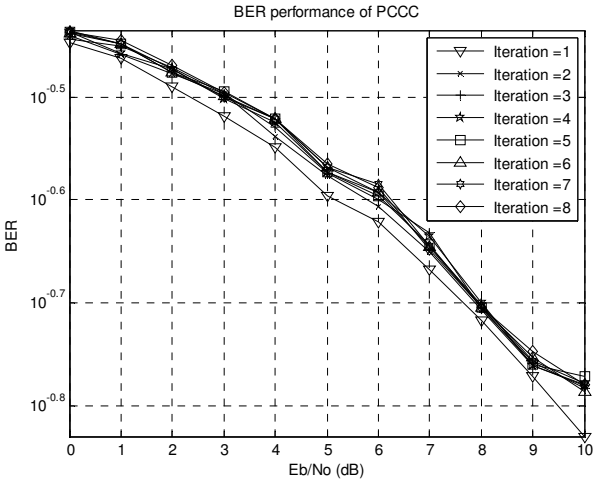

Fig. 8 BER performance for Conventional SOVA with Bayesian Gaussian Metric over SαS Channel with $\alpha = 1$.

3.3. Performance in SαS noise with Bayesian Gaussian metric

Figure 9 shows the performance of modified SOVA with Bayesian Cauchy metric. Performance improvement can be observed from the graph as SOVA iterative decoding was performed on the received data from the impulsive channel with α=1. By comparing Fig. 7 and Fig. 9, we can observe that higher E_b/N_o decoding threshold is required as the α is getting smaller. This is because smaller value of α used, the tail of SαS distribution becomes heavier and the noise is spikier in n*a*ture.

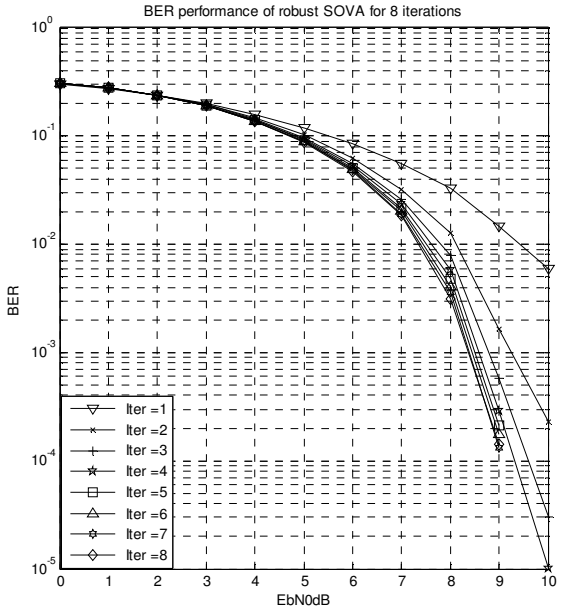

Fig. 9. BER Performance for Robust SOVA with Bayesian Cauchy Metric over SαS Channel with $\alpha = 1$.

3.4. Performance BER for different alpha at eighth iterations

The effect of different alpha values to the performance of proposed Bayesian Cauchy metric for robust SOVA decoding was studied. The BER performance is shown in Fig. 10. For ease of comparison, we choose α=1, 1.5, 1.7 and 2 for SαS noise, where α=1 is Cauchy distribution and α=2 is equivalent to Gaussian distribution.

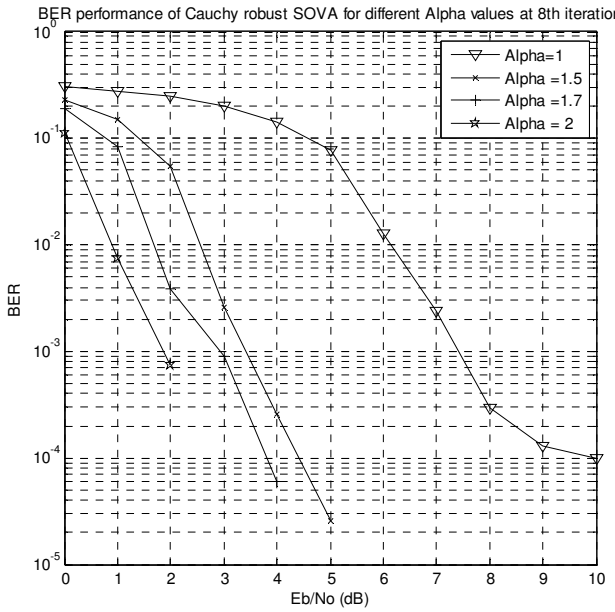

Fig. 10. BER Performance for Robust SOVA with Bayesian Cauchy Metric over SαS Channel with Different Alpha Values at 8th iteration.

Fig. 10 shows that α decreases from 2 to 1, the decoding errors of proposed Cauchy-based SOVA increase exponentially at 8th iteration from 1.9 dB to 7.5 dB in order to maintain the BER at 10^{-3}. The performance reduction is mainly due to the high degree of impulsiveness of outliers entering into proposed Cauchy-based SOVA component decoders and such outliers with smaller α typically possess larger impulses as can be seen from Fig. 3. Larger impulses present to the corrupted signal at the receiver would further distort received signals and increase the difficulty of detection as outliers. For small values of α, outliers are deviated from each other farther and cause huge discrepancy in estimation. Therefore, the required E_b/N_o would increase proportionally for proper functioning of SOVA component decoders in parallel turbo codes.

3.5. BER Comparison of Bayesian robust Log-MAP and proposed robust SOVA

Figure 11 shows the BER performance comparison for the proposed Cauchy-based robust SOVA with the previous solutions of Absolute Viterbi and Cauchy-based Log MAP decoding. The results of both Cauchy-based robust Log MAP and SOVA

turbo codes were taken at their 8th iteration. From the Fig. 11, it can be observed that robust SOVA has slightly higher BER and required additional 1 dB of coding gain to achieve the same BER ratio at 10^{-5}. However, the mathematical complexity and decoding delay for proposed robust SOVA is less complicated in comparison with robust Log MAP that has been proposed previously. Definitely, hard-decision Viterbi equipped with Absolute branch metric does not perform as good as iterative turbo codes with Log-MAP or SOVA soft decision decoding algorithms

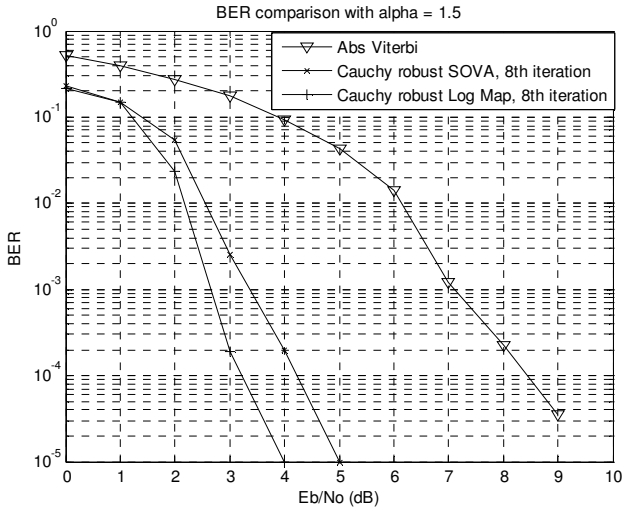

Fig. 11. BER Performance Comparison of Absolute Viterbi, Bayesian-Cauchy Robust Log Map and Bayesian-Cauchy Robust SOVA over SαS Channel with Alpha = 1.5 at 8th iteration.

4. Conclusions

In this paper, study and investigation have been carried out to enhance the detection capability of SOVA component decoders of PCCC. The introduction of Cauchy-based metric computation is proposed for iterative SOVA decoding. The implementation of such decoding procedure has been put in place and necessary changes for effective and proper functioning of Cauchy-based SOVA are described in details in this paper.

In order to ensure that such proposed system could function normally as desired under severe channel impairments of SαS noise, Mento Carlo simulation is utilized to test and find out the BER performance of the proposed robust SOVA component decoders in PCCC connection. For Gaussian-based SOVA which uses matched filtering for baseband signal detection failed to perform asymptotically to approach Shannon's predicted capacity limit in the presence of SαS noise while α less than two, and its performance decreases rapidly as α declines linearly as the noise becoming more impulsive and spiky. The reasons behind the malfunction of is due to the large value of the residuals of impulsive noise severely distorted the estimates of quadratic-type Gaussian detector in the form of match filter and its BER performance and decoded soft LLR output are shown in Figs. 5 and 8.

The Cauchy-based SOVA which exhibits monotonic logarithmic trait is found to be the remedial method to prevent the devastating effect of Gaussian-based SOVA in turbo codes in the presence of impulsive noise. Significant performance are obtained and reflected in decoded soft LLR output and BER performance curves as shown in Fig. 6, Fig. 9 and Fig. 10 respectively. Hence, the use of Cauchy-based metric has equipped the SOVA with robustness against the catastrophic residuals from the non-Gaussian channel and the turbo-like decoding of PCCC is preserved for SOVA. Therefore, the proposed incorporation of Cauchy metric into SOVA has provided another alternative pathway for practical deployment of turbo codes for modern digital communication systems over hostile transmission medium.

References

1. Shannon, C.E. (1984). Communication in the presence of noise. *Proceedings of the IEEE*, 72(9), 1192-1201.
2. Berrou, C.; Glavieux, A; and Thitimajshima, P. (1993). Near Shannon limit error-correcting coding: Turbo codes. *Proceedings of the IEEE International Conference on Communications*, 2, 1064-1070.
3. Robertson, P. (1994). Illuminating the structure of code and decoder of parallel concatenated recursive systematic (turbo) codes. *IEEE Global Telecommunications Conference*, 3, 1298 -1303.
4. Berrou, C. (2003). The ten-year-old turbo codes are entering into service. *IEEE Communications Magazine*, 41(8), 110-116.
5. Summers, T.; and Wilson, S.G. (1998). Turbo code performance in heavy-tailed noise. *Proceedings of Conference on Information Sciences and Systems*, *CISS*, 1, 495-500.
6. Barton, R.J.; and Daniel, M. (2007). Performance evaluation of non Gaussian channel estimation techniques on ultrawideband impulse radio channels. *International Journal of Communication Systems*, 20(6), 723-741.
7. Zimmermann, M.; and Dostert, K. (2002). Analysis and modeling of impulsive noise in broad-band powerline communications. *IEEE Transactions on Electromagnetic Compatibility*, 44(1), 249-258.
8. Levey, D.B.; and McLaughlin, S. (2002). The statistical nature of impulse noise interarrival times in digital subscriber loop systems. *Signal Processing*, 82(3), 329-351.
9. Chuah, T.C. (2005). Robust iterative decoding of turbo codes in heavy tailed noise. *IEE Proceedings*, 152(1), 29-38.
10. Roy, A.; and Doherty, J.F. (2008). Receiver design for turbo codes used in an impulsive noise environment. *2008 IEEE Sarnoff Symposium*, 1-5.
11. Faber, T.; Scholand, T.; and Jung, P. (2003). Turbo decoding in impulsive noise environments. *Electronic Letters*, 39(14), 1069-1071.
12. Koike, K.; and Ogiwara, H. (2001). Performance evaluation of turbo code over impulsive noise channel. *IEICE Transactions Fundamental Electronic Communications & Computer Science*, 2418-2426.

13. Zhang, L.; and Yongacoglu, A. (2002). Turbo decoding with erasures for high-speed transmission in the presence of impulse noise. *Proceedings of Zurich Seminar Broadband Communications*, Zurich, 20, 1-6.
14. Umehara, D.; Yamaguchi, H.; and Marihiro, Y. (2004). Turbo decoding in impulsive noise environment. *IEEE Global Telecommunications Conference*, 1, 194 -198.
15. Nikias, C.L.; and Shao, M. (1995). *Signal processing with alpha-stable distributions and applications*. (1st Ed.), Wiley-Interscience.
16. Chitre, M.A.; Potter, J.R.; and Ong, S.H. (2007). Viterbi decoding of convolutional codes in symmetric α-stable noise. *IEEE transactions on communications*, 55(12), 2230-2233.
17. Shehata, T.S.; Marsland, I.; and El-Tanany,M. (2010). Near optimal Viterbi decoders for convolutional codes in symmetric alpha-stable noise. *Vehicular Technology Conference*, 1-5.
18. Souryal, M.R.; Larsson, E.G.; Peric, B.; and Vojcic, B.R. (2008). Soft-decision metrics for coded orthogonal signaling in symmetric alpha-stable noise. *IEEE Transactions on Signal Processing*, 56(1), 266-273.
19. Peric, B.M.; Souryal, M.R.; Larsson, E.G.; and Vojcic, B.R. (2005). Soft decision metrics for turbo-coded FH M-FSK ad hoc packet radio networks. *Vehicular Technology Conference*, 2, 724-727.
20. Shafieipour, M; Lim, H.S.; and Chuah, T.C. (2011). Decoding of turbo codes in symmetric alpha-stable noise. *ISRN Signal Processing*, 2011(683972), 1-7.
21. Benedetto, S.; and Montorsi G. (1996). Iterative decoding of serially concatenated convolutional codes. *Electronic Letters*, 32(13), 1186-1188.
22. Hagenauer, J. (1997). The turbo principle: tutorial introduction and state of the art. *Proceedings of IEEE International Symposium on Turbo Codes and Related Topics*, 1-11.
23. Hagenauer, J.; and Hoeher, P. (1989). A Viterbi Algorithm with soft-decision outputs and its application. *IEEE Global Telecommunications Conference*, 3, 1680-1686.
24. Hanzo, L.; Liew, T.H.; and Yeap, B.L. (2002). *Turbo coding, turbo equalization and space time coding for transmission over fading channels*. John Wiley & Sons.
25. Samorodnitsky, G.; and Taqqu, M.S. (1994). *Stable non-Gaussian random processes: Stochastic models with infinite variance*. New York: Chapman & Hall.